High speed observation of damage created by a collapse of a single cavitation bubble

[1]Matevž Dular*, [1]Žan Pirc, [1]Tomaž Požar, [1]Rok Petkovšek

[1]*Faculty of Mechanical Engineering, University of Ljubljana, Askerceva 6, 1000 Ljubljana, SI-Slovenia*

Abstract

One of the remaining open questions in the cavitation erosion research is the one on the importance of the microjet and shock wave on the formation of the pit. Up until now no successful attempt was made to study this in detail, mainly because the damage could only be detected and evaluated after several successive bubble collapses. Based on our previous work on laser induced shock waves [1] and on simultaneous observation of the dynamics of cavitation clouds and cavitation damage [2], we developed a technique which enables simultaneous observation of one single cavitation bubble collapse and the damage it creates.

A bubble with a maximum diameter of up to 5 mm was formed by a Nd:YAG laser. The damage was observed on a 9 µm thick aluminum foil which was attached to the glass substrate. Two high speed cameras were simultaneously used. One captured the dynamics of the bubble, while the other recorded the damage on the foil.

We also observed the collapse of a bubble in the presence of shear flow. Most of damage was created by the microjet mechanism. Sometimes, the collapse of the bubble rim, at rebound of the initial bubble caused pits in a well-known circular pattern.

From the recordings at the very fastest acquisition rate, we determined that the material deforms and then partially relaxes, while a significant deformation remains. The whole process is only 2-3 µs long.

Keywords: caviation; erosion; single bubble; shear flow; high speed observation

1 Introduction

Currently the most widely accepted explanation for the occurrence of cavitation erosion is that the potential energy contained in a macro cavity is transformed into the radiation of acoustic pressure waves, and further on into the erosive power contained in the micro scale cavitation structures or single bubbles that collapse in the vicinity of the material boundaries [3].

Two theories describe the last stages of life of a micro-scale cavitation structure:

- the micro jet [4],
- the spherical micro bubble collapse [5].

Figure 1 schematically shows both processes.

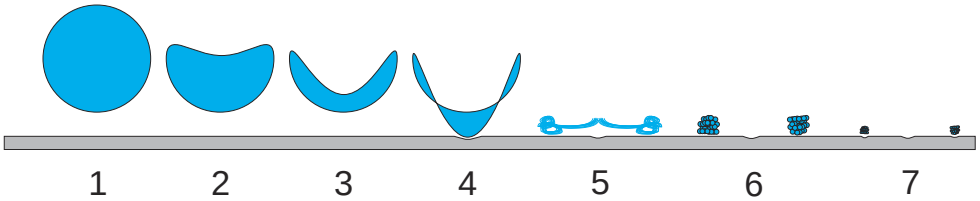

Figure 1: Two possible mechanisms of cavitation erosion.

A small bubble (mm size) reaches a higher-pressure region and becomes unstable (1). Due to the vicinity of the solid surface, its upper boundary collapses faster than the one closer to the wall (2 and 3). A microjet forms (3), which can reach a velocity of several hundred m/s. As it hits the solid surface a water hammer pressure occurs ($p=\rho cv$), which is high enough to deform the surface (4). After the microjet induced collapse, the flow moves radially outwards (5) what can cause a secondary evaporation, or "splashing" (6). This results in a number of very small bubbles, which, due to surface tension forces, preserve their spherical shape during the collapse. This results in the formation of significant shock waves, which can again reach amplitudes, capable of deforming the material (7).

*Corresponding Author, Matevz Dular: matevz.dular@fs.uni-lj.si

Which mechanism is more pronounced was until now impossible to determine directly. With the development of a novel technique, by simultaneous observation using two high speed cameras [6], the present paper investigates this issue.

2 Experiment

Experiments were performed at the Faculty of Mechanical Engineering, University of Ljubljana, Slovenia.

2.1 Experimental set-up

Figure 2 shows the schematics of the experimental set-up.

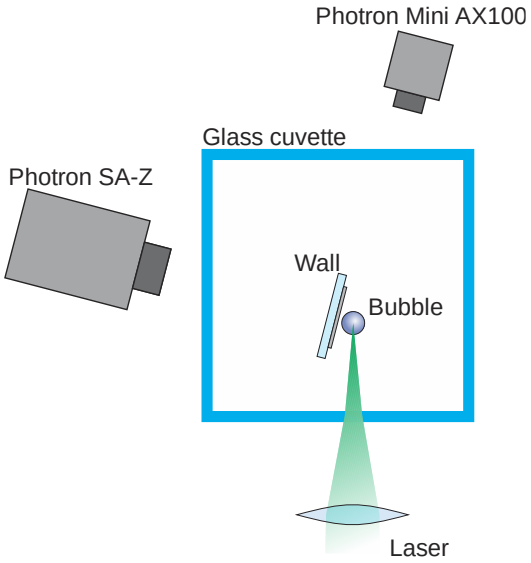

Figure 2: Experimental set-up.

A Nd:YAG laser with 1064 nm wavelenght was used to initiate the bubble growth. The energy of the 5 ns long pulse was maximally 16 mJ (10 mJ at the position of the breakdown). The focusing optics has been designed for relatively low aberrations, cone angle was 12° in water. The "standard" bubble with the diameter of 3.3 mm was generated 20 mm from the wall of the glass cuvette. The time of the bubble collapse when no wall was present was 147 μs and varied somewhat depending on the distance from the wall.

Two high speed cameras were used. Usually the slower, Photron Mini AX100, was used to observe the bubble dynamics, while the faster, Photron S-Z type 2100K-M-64GB, was used to simultaneously measure the deformation of the aluminum foil.

2.2 Aluminum foil as an erosion sensor

The idea of the experiment was to simultaneously record images of cavitation bubble and cavitation damage. The view of the upper side of the foil is obstructed by the bubble, hence one needs to look at the foil from the bottom side to see the damage. Consequently, a glass plate was used for the wall and equally important the foil had to be thin enough so that the cavitation damage which occurs on the side exposed to cavitation bubble was also visible on the other side (Fig. 3).

*Corresponding Author, Matevz Dular: matevz.dular@fs.uni-lj.si

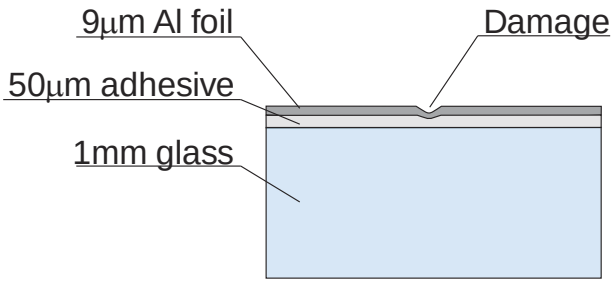

Figure 3: Construction of the "specimen".

We have chosen 9 μm thick aluminum foil and attached it to the 1mm thick glass by an optically clear two-sided adhesive tape with thickness of 50 μm (Fig. 3).

2.3 Damage detection

Since we are observing the foil with a camera, only the surface of the damaged area can be accurately measured. It is planned to estimate the geometry of the pits using stereographic and SFS (Shape From Shading) algorithms in the future [7].

For the present evaluation we used an approach that combines several evaluation procedures used before [2, 6]. We evaluated the images in pairs – the image at the time t was subtracted from the image at time t+Δt, thus eliminating most of the surface and illumination imperfections. Then we employed the pit-count method [6] which determines the pits from the darker regions in an image, while the brighter area is assumed to be undamaged surface – from each image pair we obtained the number and the area of newly appeared pits. The pit-count method gives a distribution of the number and the area of the pits and consequently, the distribution of the magnitude of cavitation erosion on the surface. We can also determine the distribution of the size of the pits. Since we were comparing pairs of two successive images we were also able to consider the possibility of pit overlapping (Fig. 4).

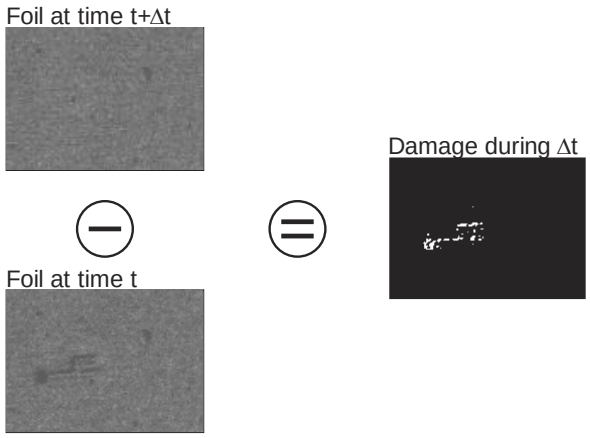

Fig. 4: Determining the damage sustained during a period of Δt.

Images of the aluminum foil were treated as matrixes A with i×j elements ($A(i,j) \in \{0,1,...255\}$) with values which can range from 0 (black) to 255 (white). Erosion was evaluated in image pairs: image matrix at time t+Δt was subtracted from image matrix at time t ($B(i,j,t) = A(i,j,t) - A(i,j,t+\Delta t)$). This way a new matrix B was obtained. When the matrix element B(i,j) did not change between times t and t+Δt its value was 0 ($B(i,j,t)=0$). When change occurred the value was $B(i,j,t)>0$. Since small changes could be present due to insignificant changes in illumination, vibration etc., damage was only considered when a certain change threshold was exceeded (more than 5% of decrease in brightness – pits always appeared as dark regions). The number of the pits, their size and overall damaged area could then be easily determined.

*Corresponding Author, Matevz Dular: matevz.dular@fs.uni-lj.si

2.4 Investigated conditions

We investigated an ensemble of conditions, where the distance of the bubble (h) from the wall was changed from $\gamma = \frac{h}{r}$ = 0.05 to 2.0. For each case 50 repetitions were made. In addition, flow was introduced in certain cases to investigate the influence of the shear forces on the specifics of bubble collapse and the induced damage.

3 Results

During the campaign we performed a vast number of experiments, which resulted in derivation of three specific cases, which are presented here in more detail. In all cases (Figs. 5 to 7) the upper sequence shows the bubble dynamics recorded by the primary camera. The bottom sequence is the result of damage evaluation (Sec. 2.3) from the images recorded by the secondary camera.

3.1 Bubble in a close vicinity of the wall (γ=0.05)

First the results of measurements in the close vicinity of the wall are presented (Fig. 5).

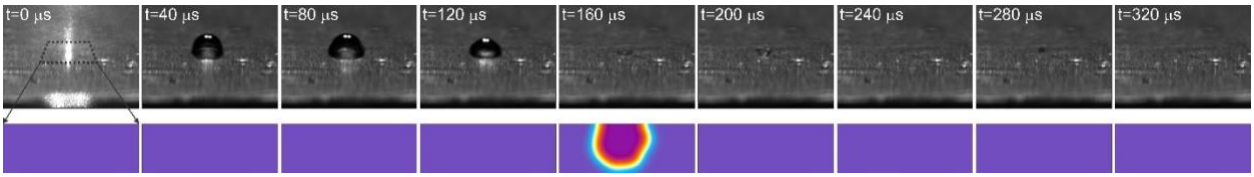

Fig. 5: Bubble and damage for collapse in the vicinity of the wall (γ=0.05)

The most pronounced damage mechanism in these cases is the micro-jet. The bubble first grows and touches the surface shortly after. The maximal size occurs about 80 µs after the laser pulse. The bubble collapses at 160 µs, and at the same instant significant damage is recorded by the second camera. The damaged area has a comparable size as the bubble shortly before the collapse, which also corresponds well to the diameter of the microjet.

3.3 Bubble in far away from the wall (γ =1.7)

Figure 6 shows the bubble and damage evolution for the case further away from the wall.

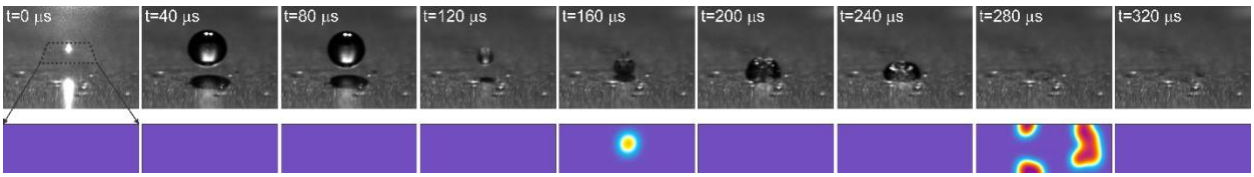

Fig. 6: Bubble and damage for collapse far away from the wall (γ =1.7)

The dynamics of the bubble is roughly the same – the same size is reached by the 80th µs but the bubble collapses a bit faster. At 160 µs the micro-jet reaches the wall and deforms it. The deformation itself is much smaller than in the case of γ =0.05 (Fig. 5). The bubble then undergoes a rebound (splashing) and a secondary collapse occurs at 280 µs. This causes significant damage in a circular pattern, which matches the diameter and the geometry of the bubble rim. One can conclude that the both mechanisms play a role in this case, but in fact the collapses of tiny bubbles inside the rim during the rebound is more aggressive.

3.4 Bubble in the presence of shear flow

Researchers argued in the past that the presence of the shear flow may significantly alter the physics of the damage occurrence. We have tested a wide range of conditions but no damage could be detected when γ exceeded 1.4 and there was no influence of the shear flow in the cases when γ was smaller than 0.5.

Fig. 7 show a representative result of this case. The flow velocity was 2.5m/s (from the right to the left) and the γ =1.0.

*Corresponding Author, Matevz Dular: matevz.dular@fs.uni-lj.si

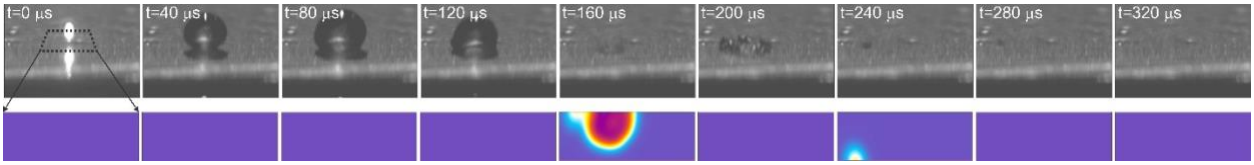

Fig. 7: Bubble and damage appearance in the presence of shear flow (γ =1.0, v=2.5 m/s)

One can see that the bubble is transported by the flow. The dynamics itself is not significantly influenced by it. The primary collapse occurs at 160 μs. The jet is deflected towards the pressure gradient by the shear forces as it was predicted by [8]. Nevertheless, its power is not diminished – it causes deformation, which is comparable to the one at stationary conditions (Fig. 5). 80 μs later, the secondary collapse occurs and causes minor damage – the position corresponds to the one of the rebounded bubble rim.

3.5 Very high-speed observation of foil deformation

To investigate further, the process of pit formation we set the camera to its fastest framerate of 2.1 Mfps. The bubble was positioned at the non-dimensional distance of γ=0.4 (without shear flow), hence we expected a single pit resulting from the micro-jet impact. Figure 8 shows the (raw) images.

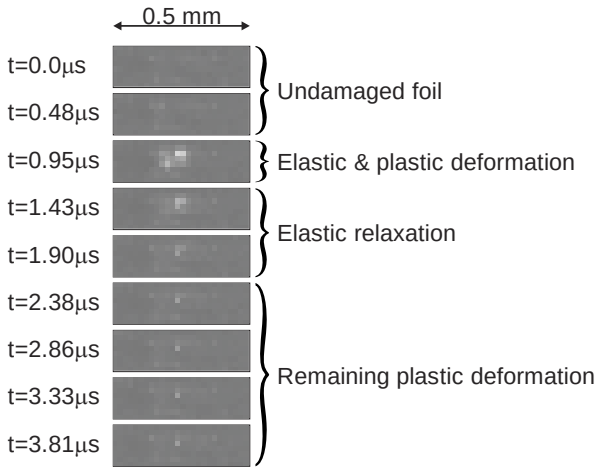

Fig. 8: Damage evolution recorded at 2.1 Mfps.

The deformation of the foil occurs in an extremely short period of time – during less than 0.5 μs. This corresponds well with the period during which the water hammer pressure is present at the jet impact. The duration of the water hammer stress is as long as the time for the impact signal to traverse the radius of the jet ($t_{wh} = \frac{r_{jet}}{c}$), which in the present case results in approximately 0.3 μs. After that time a stagnation pressure is established, which is an order of magnitude smaller than the water hammer pressure.

After the maximum deformation is reached at 0.95 μs, an elastic deformation takes place and a stationary state is established about 1.5 μs after the first contact of the micro-jet and the material.

4 Conclusions

In the study we investigated the last stage in the cascade of events that lead to the occurrence of cavitation damage – single bubble collapse and the resulting deformation of the material.

By simultaneous observation of the bubble dynamics and the deformation of a thin aluminum foil, by two high speed cameras we were able to directly observe the process.

*Corresponding Author, Matevz Dular: matevz.dular@fs.uni-lj.si

Various distances of the bubble from the specimen were investigated. We also observed the collapse of a bubble in the presence of shear flow – this was essential, since many researchers claim that the presence of a pressure gradient diminishes the erosive potential of the micro-jet.
Based on an ensemble of measurements we can conclude that:

- when cavitation bubble implodes near the wall, the most pronounced mechanism is the impact of the micro-jet;
- when the bubble collapses further away from the wall the influence of the micro-jet diminishes and the collapse of microscopic bubbles in the rebounded cloud is more important;
- finally, in the cases where the shear flow was introduced, the bubbles near the wall behaved in the same way as without the presence of the flow (micro-jet mechanism was the driving one). In the mid-range of distances ($0.5<\gamma<1.4$) the micro-jet was still the most important mechanism, but some damage was also induced by the secondary (rim) collapse and further away from the wall the deflection of the micro-jet was too large to cause either damage or rebound of the bubble.

Further on we observed the formation of a pit at the highest framerate setting of the camera and concluded that the damage indeed results from the water hammer pressure at micro-jet impact and that one can also observe deformation and relaxation of the material by this methodology.

The work represents one of the final "pieces of the puzzle", which will lead us to a detailed understanding of the cavitation erosion process and will enable development of models for prediction of cavitation damage.

Acknowledgments

The authors acknowledge the financial support from the Slovenian Research Agency (research core funding No. P2-0401 and No. P2-0270).

References

[1] R. Petkovsek, J. Mozina, and G. Mocnik, "Optodynamic characterization of shock waves after laser-induced breakdown in water.," *Optics express*, vol. 13, no. 11, pp. 4107–12, May 2005.
[2] M. Dular and M. Petkovsek, "On the mechanisms of cavitation erosion - Coupling high speed videos to damage patterns," *Experimental Thermal and Fluid Science*, vol. 68, 2015.
[3] R. Fortes-Patella, J.L. Reboud, L. Briancon-Marjollet, A phenomenological and numerical model for scaling the flow aggressiveness in cavitation erosion, EROCAV Workshop, Val de Reuil, 2004.
[4] M.S. Plesset, R.B. Chapman, Collapse of an innitially spherical vapour cavity in the neighbourhood of a solid boundary. J. Fluid Mech. 47 (1971) 283–290.
[5] R.P. Tong, W.P. Schiffers, J.S. Shaw, J.R. Blake, D.C. Emmony, The role of splashing in the collapse of the laser-generated cavity near a rigid boundary, J. Fluid Mech. 380 (1999) 339–361.
[6] M. Petkovšek, M. Dular, Simultaneous observation of cavitation structures and cavitation erosion, Wear 300 (1/2) (2013) 55-64.
[7] M. Dular, O. Coutier-Delgosha, M. Petkovsek, Observations of cavitation erosion pit formation. Ultrasonics Sonochemistry, 2013, vol. 20, iss. 4, pp. 1113-1120
[8] P.-W. Yu, S.L. Ceccio, G. Tryggvason The collapse of a cavitation bubble in shear flows-A numerical study, Phys. Fluids 7 (ll), November 1995.

*Corresponding Author, Matevz Dular: matevz.dular@fs.uni-lj.si